CRYSTAL GROWTH & DESIGN

Article

pubs.acs.org/crystal

Reactive Sputtering Deposition of Perovskite Oxide and Oxynitride Lanthanum Titanium Films: Structural and Dielectric Characterization

Published as part of the Crystal Growth & Design virtual special issue on Anion-Controlled New Inorganic Materials

Yu Lu,[†] Claire Le Paven,*[,†] Hung V. Nguyen,[†,‡] Ratiba Benzerga,[†] Laurent Le Gendre,[†] Stéphane Rioual,[§] Franck Tessier,[∥] François Cheviré,[∥] Ala Sharaiha,[†] Christophe Delaveaud,[‡] and Xavier Castel[†]

[†]Institut d'Electronique et de Télécommunications de Rennes (IETR, UMR-CNRS 6164), Equipe Matériaux Fonctionnels, IUT de Saint Brieuc, Université de Rennes 1, 18 rue Henri Wallon, 22000 Saint Brieuc, France

[‡]CEA LETI, Minatec Campus, 38054 Grenoble, France

[§]Laboratoire de Magnétisme de Brest (EA CNRS 4522), Université de Bretagne Occidentale, 29000 Brest, France

[∥]Institut des Sciences Chimiques de Rennes (ISCR, UMR-CNRS 6226), Equipe Verres et Céramiques, Université de Rennes 1, 35000 Rennes, France

Supporting Information

ABSTRACT: Perovskite lanthanum titanium thin films were deposited on Nb-doped (001) $SrTiO_3$ substrates by reactive RF magnetron sputtering using a $La_2Ti_2O_7$ target. Oxynitride $LaTiO_2N$ films were obtained using N_2 rich plasma; they display a variation of their dielectric constant as a function of DC bias in the low frequency range but not in microwaves. The dielectric constant (epsilon) values are high with, for example, epsilon = 325 at 100 kHz. The oxide films, obtained in O_2 rich plasma, are composed of an unusual $La_2Ti_2O_7$ phase with an orthorhombic cell. The films are (101) epitaxied on Nb:$SrTiO_3$ substrates. The dielectric constant value of films is around 77 with losses ~0.076 at 100 kHz; no agility of epsilon in low and high frequencies is detected. Composite and bilayer films, with oxynitride and oxide phases, exhibit a variation of epsilon under DC bias in low frequencies with, for example, an agility of 15% at 100 kHz with a maximum applied field of 40 kV/cm for the $LaTiO_2N$ (200 nm)/$La_2Ti_2O_7$ (250 nm) bilayer.

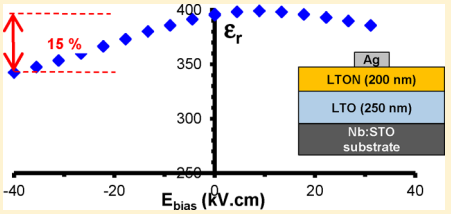

INTRODUCTION

In the field of microwaves, the need for materials with high performances drives the research on perovskite compounds, which present attractive dielectric and ferroelectric properties. In particular, the possibility of varying the dielectric constant of ferroelectric materials under the application of DC electric fields is currently studied for a use in agile components.[1] Starting from the perovskite ABO_3 type structure, one can tune the compound performance by cationic substitutions on A and/or B sites and also by anionic substitution for oxygen. That way, oxynitride perovskite compounds are obtained,[2] such as, for example, $LaTiO_2N$ from the conventional $BaTiO_3$ oxide by cross substitution of (La^{3+}, N^{3-}) from the (Ba^{2+}, O^{2-}) couple. In the form of thin films, $LaTiON_2$ can be directly prepared by PLD[3], RF-sputtering,[4] or by subsequent nitridation of an oxide film.[5] The perovskite oxynitride compounds have recently received much attention because of their unusual high dielectric constant values.[6−8] Several studies,[9−11] including first-principle calculations, are currently underway to understand the mechanism associated with this behavior and especially to find out if and how an O/N ordering, inducing the formation of highly polarizable nanopolar regions, could drive the dielectric constant.

In order to provide experimental data on dielectric properties of such compounds, we have initiated research on the deposition and characterization of $LaTiO_2N$ thin films.[12,13] The films were obtained by radio frequency (RF) reactive magnetron sputtering of an oxynitride $LaTiO_2N$ target and presented dielectric constant values of several tens to several hundred, depending on the crystalline growth of the films. Our studies also demonstrated the variation of the dielectric constant under the DC bias in the low frequency range.[14]

The purpose of the present study is to synthesize oxynitride and oxide films in the La−Ti−O−N system from the RF reactive sputtering of a $La_2Ti_2O_7$ oxide target and to evaluate their dielectric properties in low and high frequencies. It also introduces the deposition and characterization of original multilayer structuration, such as composite and bilayer films containing oxynitride and oxide phases.

Received: July 5, 2013
Revised: September 23, 2013
Published: October 17, 2013

Table 1. Deposition Parameters and Characteristics of Oxynitride (LTON) and Oxide (LTO) Thin Films Deposited by Reactive RF Magnetron Sputtering of a $La_2Ti_2O_7$ Target

film	substrate	reactive gas	thickness (nm)	ε' (100 kHz, RT)	tan δ (100 kHz, RT)	ε' (10 GHz, RT)	tan δ (10 GHz, RT)
LTON-1	Nb:$SrTiO_3$	50% N_2	300	375	1.000	60	0.200
LTON-2	MgO		–	–	–	–	–
LTO-1	Nb:$SrTiO_3$	25% O_2	510	77	0.076	62	0.011
LTO-2	$LaAlO_3$		–	–	–	–	–
LTO-3	$SrTiO_3$		–	–	–	–	–
C-1	Nb:$SrTiO_3$	5% N_2	250	600	1.800	–	–
B-1	Nb:$SrTiO_3$	25% O_2/50% N_2	450	400	0.500	–	–

EXPERIMENTAL SECTION

Thin films were grown by radio frequency reactive magnetron sputtering, using a homemade $La_2Ti_2O_7$ target. The latter was realized by a uniaxial compaction of powder under 32 MPa. No sintering was performed. The compacted powder target measures 75 mm in diameter and 2.5 mm in thickness. The starting $La_2Ti_2O_7$ powder used for making the target was prepared by molten salt synthesis.[15] In brief, La_2O_3 and TiO_2 precursors were mixed in a 1:2 mol ratio. A salt consisting of 50 mol % NaCl and 50 mol % KCl was then added, constituting 50 wt % of the total reaction mixture. The corresponding mixture was heated at 1000 °C for 15 h. The resulting product was washed using distilled water, dried, and clearly identified as the monoclinic $La_2Ti_2O_7$ compound by X-ray diffraction.

The films were deposited on (001) Nb:$SrTiO_3$ substrates, chosen for its small crystallographic mismatch with the deposited compounds, as well as its electric conductive character. This way, the substrate itself serves as the lower conducting electrode of the MIM (metal−insulator−metal) structure used for the dielectric measurements. The upper electrodes are constituted by concentric silver metallic disks, obtained by standard photolithography and wet etching process of a metallization layer (2 μm Ag/5 nm Ti) deposited by sputtering. In high frequencies, the MIM structure corresponds to two capacities in series with a floating bottom electrode.[16]

For the thin film deposition, the reactive gas mixture (argon + N_2 or O_2) was introduced in the chamber after the base pressure reaches a value of 10^{-3} Pa. The gas purities were 99.9996% for Ar, 99.9999% for N_2, and 99.9995% for O_2. During deposition, the total pressure was kept at 3.6 Pa and the ratio of reactive gas in the sputtering gas was fixed at 25 or 50% (vol %). The input power on the target was 100 W (power density 2.26 W/cm^2). The temperature of the substrate holder (T_S) was set at 800 °C during the deposition processes. The distance between substrate and target was fixed at 5 cm. After deposition, cooling was performed at 10 °C min^{-1} in the deposition atmosphere. No post annealing was performed.

Several samples were deposited for this study; the deposition parameters and characteristics of studied films are given in Table 1. The oxynitride (LTON) films were prepared using a nitrited $La_2Ti_2O_7$ target that is a target presputtered and sputtered with 50 vol % N_2 in the plasma. The oxide (LTO) films were obtained with the $La_2Ti_2O_7$ target presputtered and sputtered in plasma containing 25 vol % O_2. Furthermore, samples containing LTON and LTO were synthesized in the form of a composite (C) and a bilayer (B) films. The C-1 sample was deposited using the $La_2Ti_2O_7$ target sputtered with 5 vol % N_2, which means with a target being nitrided during the deposition. The B-1 bilayer was deposited in two runs: the first one, for the deposition of the oxide layer, with the target presputtered and sputtered under 25 vol % O_2, and the second one, for the deposition of the oxynitride layer, with the target presputtered and sputtered under 50 vol % N_2.

The chemical composition of samples was determined by semi-quantitative energy dispersive spectrometry (EDS) in a JEOL 5440 scanning electron microscope (SEM), operating at 10 kV. Some samples were also characterized by X-ray photoelectron spectrometry (XPS) with the apparatus detailed in ref [17]. In order to protect the surfaces from any contamination before XPS analysis, the samples were ex situ-coated by 5 nm of gold just after their deposition. X-ray diffraction (XRD) analysis was performed on a Seifert 3003 PTS diffractometer (Cu Kα1 radiation). Stereotypes electron channeling patterns (ECP) were recorded on a conventional Jeol JSM 6400 SEM, operating at 25 kV. Cross-section observations were conducted using a JEOL 5440 SEM; the error in the thickness value is estimated at 10 nm.

The dielectric characteristics (dielectric constant ε' and dielectric losses tan δ) were obtained, in the low frequency range, using a RLC bridge and an Instek LCR819 impedance analyzer and, in high frequency range, using a HP8510C network analyzer associated to a Signatone H100 probe station. In both cases, a stabilized Keithley 2400 supply was used to provide a DC electric field in order to determinate the agility of the films. The latter is defined as agility (%) = $|\varepsilon'_{E=Emax} - \varepsilon'_{E=0}/\varepsilon'_{E=0}|$ or $|C_{E=Emax} - C_{E=0}/C_{E=0}|$, where C is the measured capacitance of the MIM structure and E the applied DC field.

RESULTS AND DISCUSSION

With concern for the chemical composition of films, the EDS analysis gave a nitrogen content of 20% for the LTON-1 sample, whereas no nitrogen was detected in the LTO-1 film. The analysis also shows a La/Ti ratio almost equal to 1 for the two films. To confirm these values, XPS experiments were performed on additional samples deposited in the same conditions on the MgO substrate for an oxynitride film (LTON-2) and on the $LaAlO_3$ substrate for an oxide film (LTO-2). Figure 1 shows the spectra related to the La(4p), Ti(2p), O(1s), and N(1s) contributions of both samples. Clearly, the presence of nitrogen is confirmed in the oxynitride film; the peak at 397.1 eV is the characteristic nitride ion fingerprint[18] and confirms the substitution of nitrogen for oxygen in the perovskite cell. A shoulder at 399 eV can be associated to the N−H surface species.[19] No nitrogen is detected in the oxide sample. The O 1s peak intensities at 530.5 eV shows that the oxygen content is lower in the LTON-2 sample than in the LTO-2 one, as expected in view of the chemical composition of $LaTiO_2N$ (O = 40 at. %) and $La_2Ti_2O_7$ (O = 63.6 at. %). In both cases, a shoulder on the O peak is observed at the high binding energy, which is characteristic of the presence of OH groups on the surface of films. The La and Ti peak shapes are nearly identical for the oxynitride and oxide films. In particular, the Ti 2p3/2 peaks are centered at 458.7 eV, characteristic of Ti^{4+} contributions.[20] No trace of the shoulder at lower values corresponding to Ti^{3+} ions can be observed. Furthermore, from the peak intensities, and considering the *LTON-2* film as a reference with a ratio La/Ti = 1 (regarded as the $LaTiO_2N$ formulation which will be confirmed by XRD in the next section), we calculated a La/Ti ratio of 1.02 for the oxide LTO-2 film. These results, in correlation with the EDS analysis, show that the LTON and LTO deposited films are Ti^{4+}-containing oxynitride and oxide compounds with a La/Ti ratio close to 1.

The Figure 2a presents the $\theta-2\theta$ diffractogram recorded on the LTON-1 sample. Weak peaks are observed; the 2θ position indexation can be done using a tetragonal $LaTiO_2N$ phase (JCPDS 48-1230). The film is slightly textured along its c axis on

dx.doi.org/10.1021/cg4010196 | Cryst. Growth Des. 2013, 13, 4852−4858

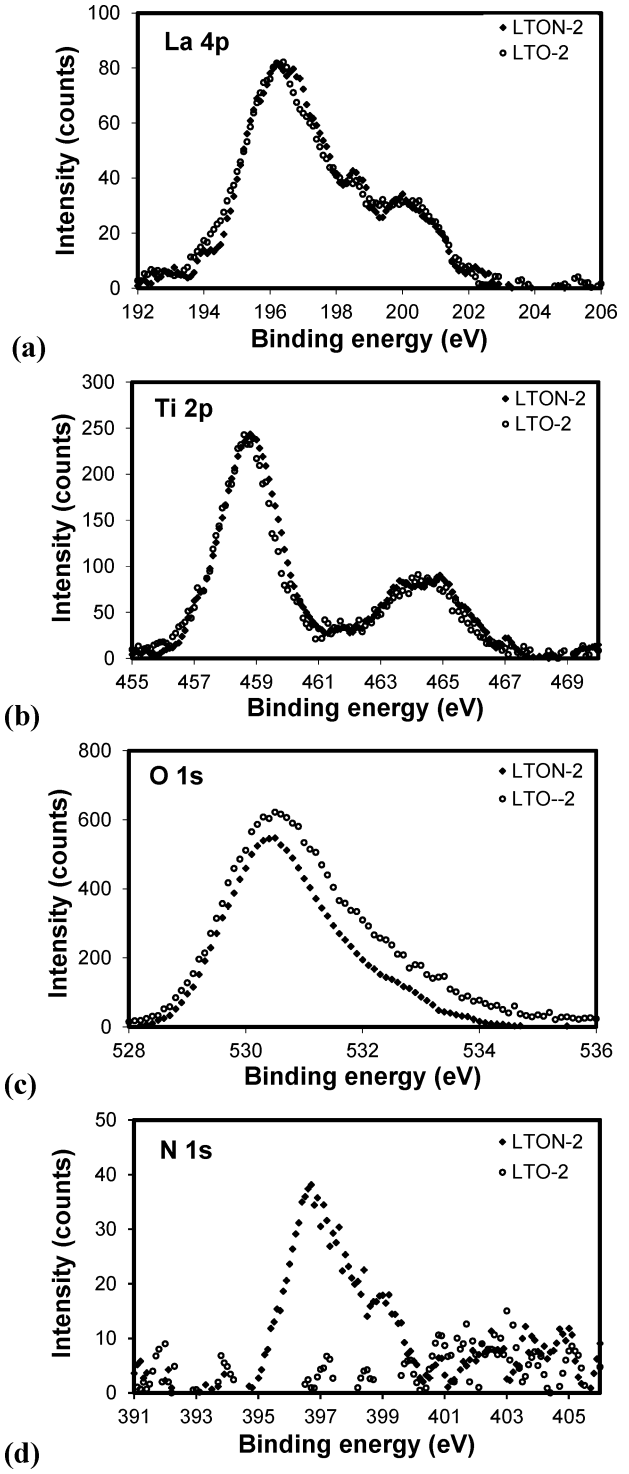

Figure 1. (a-d) X-ray photoelectron spectroscopy (XPS) La(4p), Ti(2p), O(1s), and N(1s) narrow scans of the LTON-2 and LTO-2 films deposited on MgO and $LaAlO_3$ substrates by RF reactive magnetron sputtering at T_S = 800 °C and % N_2 = 50 and % O_2 = 25, respectively.

the (001) Nb:$SrTiO_3$ substrate. No evidence of the other phase is found. The oxide LTO-1 sample exhibits relatively intense diffracted peaks in addition to those of substrate and silver metallization, as observed in Figure 2b. The low value of the rocking curve performed on the more intense peak ($\Delta\theta = 0.30°$) reveals that the peaks are related to an orientation of the film on

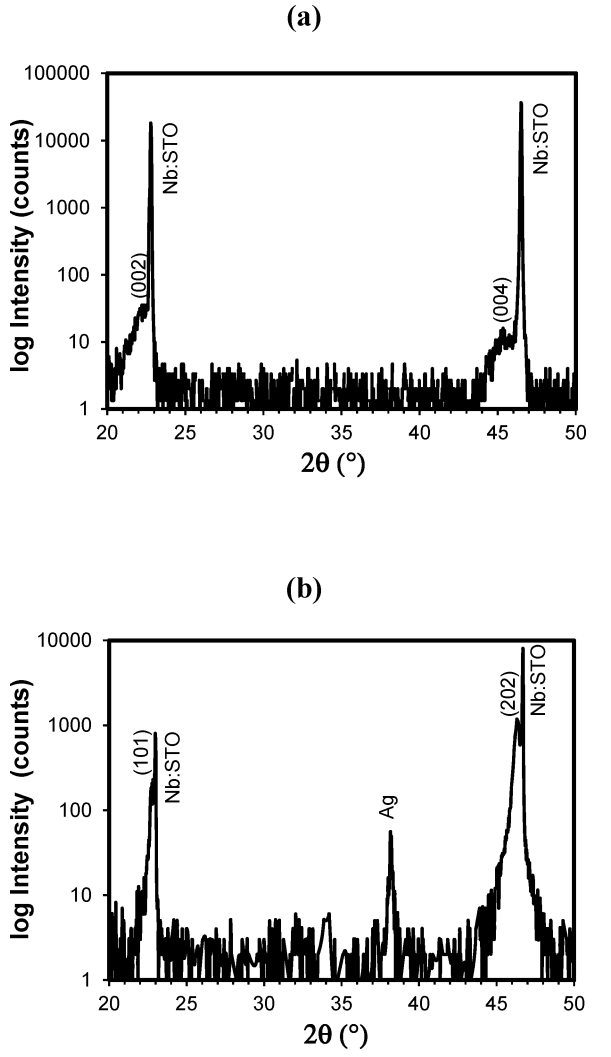

Figure 2. θ–2θ X-ray diffractogramms registered on (a) LTON-1 film and (b) LTO-1 film, deposited on (001) Nb:$SrTiO_3$ substrates by RF reactive magnetron sputtering at T_S = 800 °C and % N_2 = 50 and % O_2 = 25, respectively.

the (001) Nb:$SrTiO_3$ substrate. The experimental 2θ angular positions show neither valuable match with the listed monoclinic $La_2Ti_2O_7$ compound (JCPDS 81-1066) nor the $La_2Ti_2O_7$ thin films studied in literature.[21,22] With the assumption that a La/Ti = 1 formulation with Ti^{4+} ions and the fact that depositions are made using a $La_2Ti_2O_7$ target under oxygen rich plasma, we propose to identify the deposited oxide as the unusual orthorhombic $La_2Ti_2O_7$ phase with a space group $Cmc2_1$, as proposed by Ishizawa for single crystals at temperature above 780 °C.[23] No JCPDS file exists for this orthorhombic phase, but one can be found for a perovskite oxide analogue, the orthorhombic $Sr_2Ta_2O_7$ phase with the $Cmc2_1$ space group (JCPDS 72-0921). From the latter file, the LTO-1 diffracted peaks can be indexed as (101) and (202), with a weak angular deviation with the calculated 2θ values obtained from the reported crystallographic parameters (a = 3.954 Å, b = 5.607 Å, and c = 25.952 Å).[23] Furthermore, the very low lattice mismatch (−0.1%) with $SrTiO_3$ substrate makes possible an epitaxial growth of the LTO films. Indeed, the epitaxy is confirmed by electron channeling pattern on another film (LTO-3) deposited on the (001) $SrTiO_3$ substrate with the same deposition conditions than the previous samples: the ECP shows the appearance of a cross (see the

dx.doi.org/10.1021/cg4010196 | Cryst. Growth Des. 2013, 13, 4852−4858

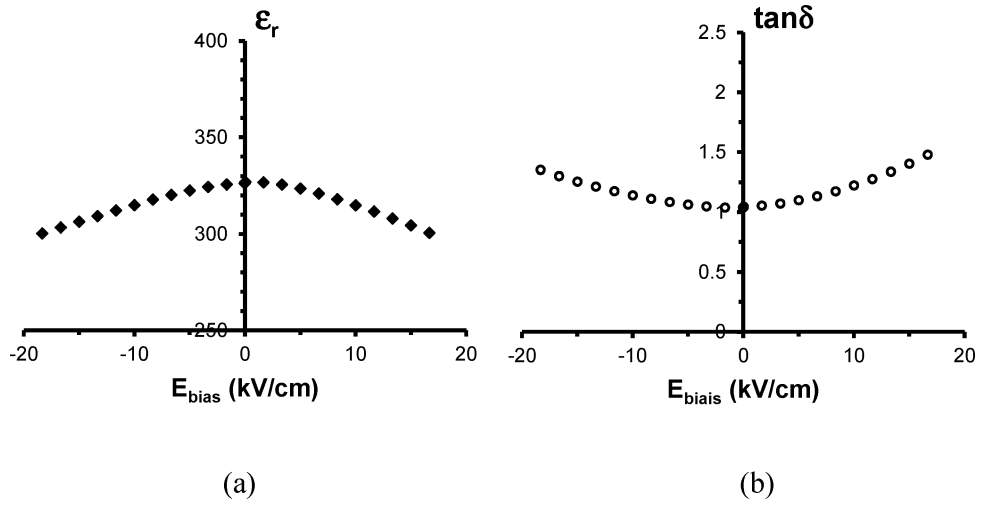

Figure 3. (a) Dielectric constant (ε') and (b) loss tangent (tan δ) of oxynitride LTON-1 film as a function of the DC electric field at 100 kHz and room temperature.

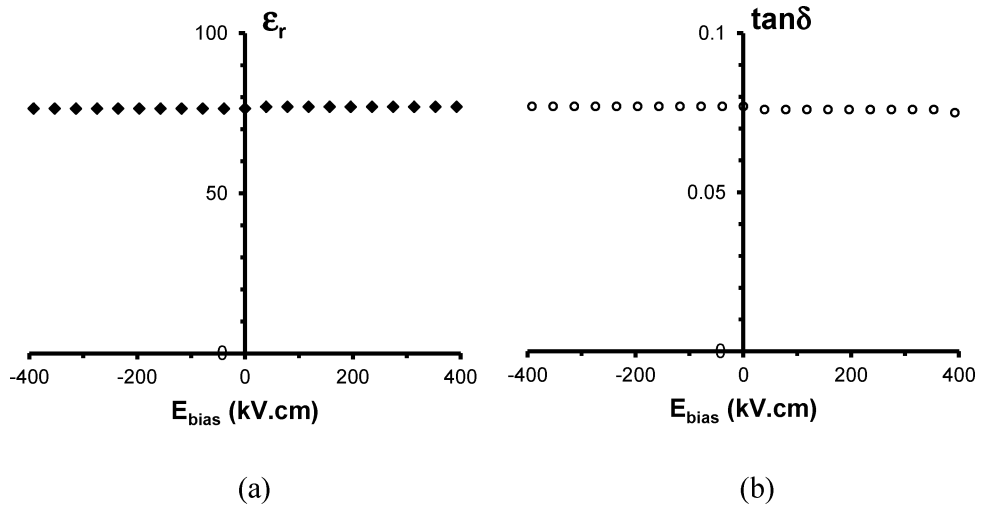

Figure 4. (a) Dielectric constant (ε') and (b) loss tangent (tan δ) of oxide LTO-1 film as a function of the DC electric field at 100 kHz and room temperature.

Supporting Information), indicating a three-dimensional arrangement of atoms in the film.[24] Although such an analysis was not made on the LTO-1 sample, we assume an epitaxial growth for the latter. The orthorhombic $La_2Ti_2O_7$ phase has never been reported as thin films at ambient temperature, but as previously said, an analog exists for the $Sr_2Ta_2O_7$ compound in bulk and thin films.[25] In our case, the high-energy sputtering deposition method stabilizes the phase at low temperature. Its formation is also enhanced by the high crystallographic interaction with the substrate as the present films are epitaxied.

The Figures 3 and 4 display the evolution of the dielectric constant (ε') and dielectric losses (tan δ), according to the DC applied electric field, at 100 kHz and room temperature, for the LTON-1 and LTO-1 samples, respectively. The oxynitride LTON-1 film shows a variation of ε' and tan δ, with an agility value of 8% for a maximum applied field of 16.7 kV/cm (above, the film is too conducing) and losses in excess of 1. These losses are high, so that the oxynitride compound cannot be used in this form in agile devices; the observed increase of tan δ with an applied DC field hints that a part of the losses may be linked to space charge phenomenon and/or anionic vacancies. The dielectric constants are high with a maximum of 325. This feature is in accordance with studies on oxynitride perovskite compounds,[6−8] evidencing high dielectric constant values for these materials compared to their oxide parents. The dielectric characteristics of the oxide LTO-1 film are remarkably stable with the DC applied field, with a dielectric constant of 77 and losses of 0.076 (100 kHz, RT), which also implies that this compound is not agile in low frequencies (maximum applied field = 400 kV/cm). Measurements were performed in the high frequency range, up to 20 GHz, but no result can be obtained for the oxynitride LTON-1 film because it becomes conducting as soon as a DC field is applied. The measurement is possible on the oxide LTO-1 sample, but again, no variation under DC bias can be detected (see the Supporting Information). At 10 GHz, the dielectric characteristics of the oxide film are $\varepsilon' = 62$ and tan $\delta = 0.011$. At zero bias and 10 GHz, the characteristics of the oxynitride LTON-1 film are $\varepsilon' = 60$ and tan $\delta = 0.20$.

The above results point out that the $LaTiO_2N$ compound is agile in low frequencies, but not in high frequencies, and finally can be considered as a semiconductor rather than an insulator. This result can be related to its band gap value (close to 2.5 eV)[12] and its high dielectric losses. The orthorhombic $La_2Ti_2O_7$ compound is an insulator, with very low dielectric losses, but

dx.doi.org/10.1021/cg4010196 | Cryst. Growth Des. 2013, 13, 4852−4858

our study shows no agility or ferroelectric behavior of this material at room temperature in low and high frequencies. Depositions were thus conducted to prepare composite and bilayer films, that is to say samples composed of the oxynitride phase showing tunability and of the oxide phase presenting low losses. The EDS analysis of composite C-1 film gives a nitrogen content of 4.5%, which must be taken as an average content in the sample. Indeed, the $\theta-2\theta$ diffractogram (Figure 5a) shows two

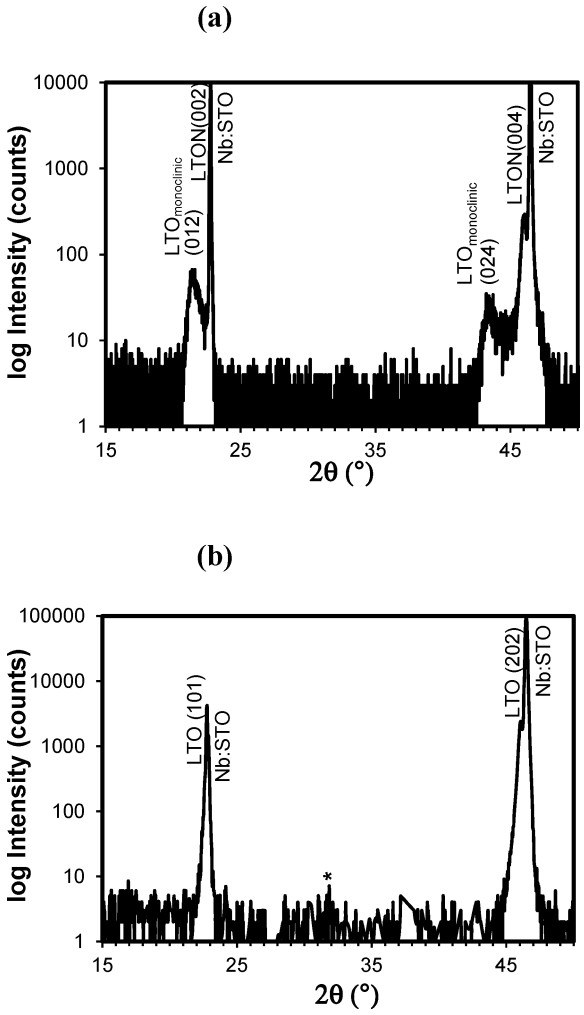

Figure 5. $\theta-2\theta$ X-ray diffractogramms registered on (a) composite C-1 film and (b) bilayer B-1 film deposited on (001) Nb:$SrTiO_3$ substrates by reactive magnetron sputtering at T_S = 800 °C. The weak peak marked by an asterisk in (b) can be attributed to an oxynitride contribution corresponding to the LTON (112) plane.

sets of peaks: a series corresponding to the oxynitride $LaTiO_2N$ phase, with a *c* axis orientation, and a second series which can be assigned to the monoclinic $La_2Ti_2O_7$ phase, with a (012) orientation. So, the C-1 film is a mixture of lanthanum titanium oxide and oxynitride compounds. The EDS analysis of bilayer B-1 sample indicates an average nitrogen content of 17%. The $\theta-2\theta$ diffractogram (Figure 5b) reveals that the sample is a mixture of an oxynitride phase, with a polycrystalline contribution [the only visible peak is the more intense $LaTiO_2N$ (112) peak] and an oxide orthorhombic $La_2Ti_2O_7$ phase (the new one proposed in this article), with a (101) orientation. The cross-section SEM observation confirms that the B-1 sample is actually a bilayer; thicknesses of 250 and 200 nm are measured, respectively, for the oxide layer and the oxynitride layer.

Figures 6 and 7 show the variation of ε' and tan δ as a function of an applied DC electric field, at 100 kHz and RT, for the composite C-1 and bilayer B-1 samples, respectively. The composite film shows an agility of 13% for a maximum electric field of 5 kV/cm. Its dielectric characteristics (ε', tan δ) are higher than those of single LTON-1 film, suggesting that this sample may contain nitrogen-induced defects responsible for high polarization but also for high losses. The bilayer film displays improved values compared to single oxynitride film, with an agility of 15% for a maximum electric field of 40 kV/cm and dielectric losses around 0.5. The maximum dielectric constant (400) is higher than the one of single oxynitride film and losses are reduced by a factor of 2. This result is promising; improvements have to be made to further reduce the dielectric loss and integrate the LTO and LTON materials in frequency agile devices such as antennas.[16]

Finally, regarding the current studies on oxynitride perovskite compounds, our results suggest that $LaTiO_2N$ is not a (classical) ferroelectric material: its dielectric losses are much higher than the ones of oxide ferroelectric compounds (for example, ref 26), and the losses increase with DC bias and no agility is obtained in high frequencies. Nevertheless, its dielectric constant is high and varies under DC bias in the low frequency range. As underlined by several studies on ABO_2N compounds (mostly as bulk materials),[6−8] the high dielectric constant values obtained for oxynitride perovskite materials may be caused by the existence of nanopolar regions, related to an ordering of oxygen and nitrogen ions in the perovskite stack. Our experimental contribution shows that high permittivities are actually obtained for $LaTiO_2N$ films and related samples (composite, bilayer); it also suggests that the mechanism responsible for the permittivity variation in low frequencies is ineffective in high frequencies.

■ CONCLUSION

Perovskite oxide and oxynitride films were deposited by reactive magnetron RF sputtering of a $La_2Ti_2O_7$ powdered target. Under N_2 rich plasma, tetragonal $LaTiO_2N$ films are obtained with a slight *c* axis orientation on Nb-doped (001) $SrTiO_3$ substrate. XPS experiments confirm the presence of nitrogen in samples with a characteristic fingerprint of a nitride ion. The oxynitride film exhibits agility of its dielectric constant under the DC electric field in the low frequency range but not in microwaves. Under O_2 rich plasma, an unusual lanthanum titanium oxide is deposited, which we identify as an orthorhombic $La_2Ti_2O_7$ phase with a (101) orientation on the (001) Nb:$SrTiO_3$ substrate. The film does not show variation of its dielectric constant under the DC electric field in low and high frequencies. Mixtures of oxide and oxynitride phases were engineered in the form of single and bilayer films. The $LaTiO_2N/La_2Ti_2O_7$ bilayer shows the highest agility in low frequencies with a value of 15% at 100 kHz (applied field 40 kV/cm). Optimization is under work to further reduce the losses and increase applied DC fields. Our experimental study finally suggests that the perovskite $LaTiO_2N$ compound does not behave as a classical ferroelectric but contains polar entities active in low frequencies and responsible for the observed high dielectric constant values and their variation under DC electric fields.

dx.doi.org/10.1021/cg4010196 | *Cryst. Growth Des.* 2013, 13, 4852−4858

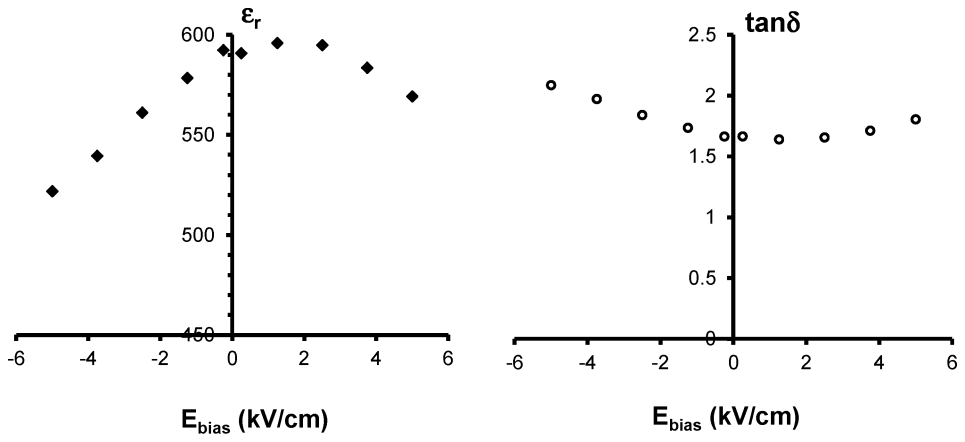

(a) (b)

Figure 6. (a) Dielectric constant (ε') and (b) loss tangent (tan δ) of composite C-1 film, as a function of the DC electric field at 100 kHz and room temperature.

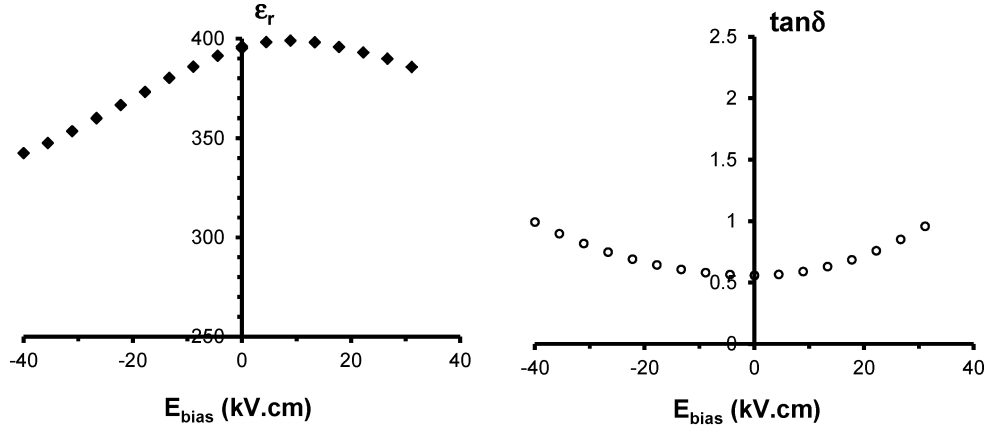

(a) (b)

Figure 7. (a) Dielectric constant (ε') and (b) loss tangent (tan δ) of bilayer B-1 film as a function of the DC electric field at 100 kHz and room temperature.

■ ASSOCIATED CONTENT

Supporting Information

Electron channeling pattern of the LTO-3 film deposited on (001)$SrTiO_3$ substrate by reactive magnetron sputtering at T_S = 800 °C and % O_2 = 25 and variation of the capacitance of a MIM structure on the LTO-1 film as a function of frequency for two DC electric fields. This material is available free of charge via the Internet at http://pubs.acs.org.

■ AUTHOR INFORMATION

Corresponding Author

*E-mail: claire.lepaven@univ-rennes1.fr. Tel: 33-(0)296609659. Fax: 33-(0)296609652, http://www.ietr.fr.

Notes

The authors declare no competing financial interest.

■ ACKNOWLEDGMENTS

The authors gratefully acknowledge the Region Bretagne, CNRS, and CEA for thesis financial support, and S. Casale and J. Le Lannic of Rennes 1 University for the ECP experiments.

■ REFERENCES

(1) Gevorgian, S.; Vorobiev, A.; Deleniv, A. Ferroelectrics in microwave devices, circuits and systems physics, modeling, fabrication and measurements. In *Engineering Materials and Processes*; Springer: London, 2009; pp 61−113.

(2) Tessier, F.; Marchand, R. *J. Solid State Chem.* **2003**, *171*, 143−151.

(3) Marozau, I.; Shkabko, A.; Döbeli, M.; Lippert, T.; Mallepell, M.; Schneider, C. W.; Weidenkaff, A.; Wokaun, A. *Acta Mater.* **2011**, *59*, 7145−7154.

(4) Le Paven-Thivet, C.; Le Gendre, L.; Le Castrec, J.; Chevire, F.; Tessier, F.; Pinel. *Prog. Solid State Chem.* **2007**, *35*, 299−308.

(5) Aguiar, R.; Weidenkaff, A.; Schneider, C. W.; Reller, A.; Ebbinghaus, S. G. *Prog. Solid State Chem.* **2007**, *35*, 291−298.

(6) Kim, Y. I.; Woodward, P. M.; Baba-Kishi, K. Z.; Tai, C. W. *Chem. Mater.* **2004**, *16*, 1267−1276.

(7) Kim, Y. I.; Si, W.; Woodward, P. M.; Sutter, E.; Park, S.; Vogt, T. *Chem. Mater.* **2007**, *19*, 618−623.
(8) Zhang, Y.-R.; Motohashi, T.; Masubuchi, Y.; Kikkawa, S. *J. Ceram. Soc. Jpn.* **2011**, *119*, 581−586.
(9) Fang, C. M.; de Wijs, G. A.; Orhan, E.; de With, G.; de Groot, R. A.; Hintzen, H. T.; Marchand, R. *J. Phys. Chem. Solids* **2003**, *64*, 281−286.
(10) Page, K.; Stoltzfus, M. W.; Kim, Y.-I.; Proffen, T.; Woodward, P. M.; Cheetham, A. K.; Seshadri, R. *Chem. Mater.* **2007**, *19*, 4037−4042.
(11) Yang, M.; Oro-Sole, J.; Rodgers, J. A.; Jorge, A. B.; Fuertes, A.; Attfield, J. P. *Nat. Chem.* **2011**, *3*, 47−52.
(12) Lu, Y.; Ziani, A.; Le Paven-Thivet, C.; Benzerga, R.; Le Gendre, L.; Fasquelle, D.; Kassem, H.; Tessier, F.; Vigneras, V.; Carru, J.-C.; Sharaiha, A. *Thin Solid Films* **2011**, *520*, 778−783.
(13) Ziani, A.; Le Paven-Thivet, C.; Fasquelle, D.; Le Gendre, L.; Benzerga, R.; Tessier, F.; Cheviré, F.; Carru, J. C.; Sharaiha, A. *Thin Solid Films* **2012**, *520*, 4536−4540.
(14) Fasquelle, D.; Ziani, A.; Le Paven-Thivet, C.; Le Gendre, L.; Carru, J. C. *Mater. Lett.* **2011**, *65*, 3102−3104.
(15) Fuierer, P. A.; Newham, R. E. *J. Am. Ceram. Soc.* **1991**, *74*, 2876−2881.
(16) Nguyen, H.; Benzerga, R.; Delaveaud, C.; Sharahia, A.; Lu, Y.; Le Paven-Thivet, C.; Le Gendre, L.; Castel, X., *Proceedings of the 6th European Conference on Antennas and Propagation (EUCAP)*, Prague, Czech Republic, March 26 − 30, 2012; IEEE: Piscataway, NJ, 2012.
(17) Salou, M.; Lescop, B.; Rioual, S.; Lebon, A.; Ben Youssef, J.; Rouvellou, B. *Surf. Sci.* **2008**, *602*, 2901−2906.
(18) Masuda, Y.; Mashima, R.; Mayada, M.; Ikeuchi, K.; Murai, K.; Waterhouse, G. I. N.; Metson, J. B.; Moriga, T. *J. Ceram. Soc. Jpn.* **2009**, *117*, 76−81.
(19) Oja Acik, I.; Kiisk, V.; Krunks, M.; Sildos, I.; Junolainen, A.; Danilson, M.; Mere, A.; Mikli, V. *Appl. Surf. Sci.* **2012**, *261*, 735−741.
(20) Atuchin, V. V.; Gravilova, T. A.; Grivel, J.-C.; Kesler, V. G. *J. Phys. D: Appl. Phys.* **2009**, *42*, 035305−035311.
(21) Ohtomo, A.; Muller, D. A.; Grazul, J. L.; Hwang, H. Y. *Appl. Phys. Lett.* **2002**, *80*, 3922−3924.
(22) Shao, Z.; Saitzek, S.; Roussel, P.; Huvé, M.; Desfeux, R.; Mentré, O.; Abraham, F. *J. Cryst. Growth* **2009**, *311*, 4134−4141.
(23) Ishizawa, N.; Marumo, F.; Iwai, S.; Kimura, M.; Kawamura, T. *Acta Crystallogr., Sect. B* **1982**, *38*, 368−372.
(24) Perrin, A.; Guilloux-Viry, M.; Thivet, C.; Jegaden, J. C.; Sergent, M.; Le Lannic, J. *JEOL News* **1992**, *2*, 26−29.
(25) Okuwada, K.; Nakamura, S.-I.; Nozawa, H. *J. Mater. Res.* **1999**, *14*, 855−860.
(26) Levasseur, D.; El-Shaarawi, H. B.; Pacchini, S.; Rousseau, A.; Payan, S.; Guegan, G.; Maglione, M. *J. Eur. Ceram. Soc.* **2013**, *33*, 139−146.